Available online at www.sciencedirect.com

SciVerse ScienceDirect

journal homepage: www.elsevier.com/locate/he

Mechanistic aspects of the low temperature steam reforming of ethanol over supported Pt catalysts

*Paraskevi Panagiotopoulou**, *Xenophon E. Verykios*

Department of Chemical Engineering, University of Patras, University Campus, Rio, GR-26504 Patras, Greece

ARTICLE INFO

Article history:
Received 18 November 2011
Received in revised form
13 February 2012
Accepted 15 February 2012
Available online 14 March 2012

Keywords:
Ethanol steam reforming
Water-gas shift
Platinum
Metal oxide
FTIR
Transient-MS

ABSTRACT

The influence of the support of Pt catalysts for the reaction of steam reforming of ethanol at low temperatures has been investigated on Al_2O_3, ZrO_2 and CeO_2. It was found that the conversion of ethanol is significantly higher when Pt is dispersed on Al_2O_3 or ZrO_2, compared to CeO_2. Selectivity toward H_2 is higher over ZrO_2-supported catalyst, which is also able to decrease CO production via the water-gas shift reaction. Depending on catalyst employed, interaction of the reaction mixture with the catalyst surface results in the development of a variety of bands attributed to ethoxy, acetate and formate/carbonate species associated with the support, as well as by bands attributed to carbonyl species adsorbed on platinum sites. The oxidation state of Pt seems to affect catalytic activity, which was found to decrease with increasing the population of adsorbed CO species on partially oxidized ($Pt^{\delta+}$) sites. Evidence is provided that the main reaction pathway ethanol dehydrogenation, through the formation of surface ethoxy species and subsequently acetaldehyde, which is decomposed toward methane, hydrogen and carbon oxides. The population of adsorbed surface species, as well as product distribution in the gas phase varies significantly depending on catalyst reactivity towards the WGS reaction.

1. Introduction

Recent developments indicate that, in the near future, hydrogen will be used, to a large extent, as a secondary energy carrier for the production of electricity for mobile and small-to-medium scale stationary applications [1,2]. Among the various technologies which have been proposed for production of hydrogen, steam reforming of ethanol (Eq. (1)) seems to be attractive, economically and environmentally, since ethanol can be produced from renewable biomass [2–6].

$$C_2H_5OH + 3H_2O \rightarrow 6H_2 + 2CO_2 \quad \Delta H^{\circ}_{298} = 196.7\ kJ/mol \qquad (1)$$

Depending on the catalyst used and operating conditions employed, several reactions may run in parallel, such as ethanol decomposition, dehydrogenation and dehydration, methane reforming, water-gas shift (WGS) and hydrogenation reactions producing acetaldehyde, hydrogen, methane, carbon oxides and ethylene [7].

One of the major problems in ethanol steam reforming is coke formation on the catalyst surface, which may take place via several processes, such as the "Boudouard" reaction [2], methane decomposition [8] and cracking of ethylene produced by dehydration of ethanol [2,7]. Carbon deposition can be avoided at high temperatures, where high hydrogen yield can also be achieved [4,8]. However, high reaction temperatures enhance the formation of byproduct CO, due to the thermodynamically favored reverse WGS and dry methane reforming reactions. For PEM fuel cell applications,

* *Corresponding author*. Tel./fax: +30 2610 991527.
E-mail address: ppanagiotopoulou@chemeng.upatras.gr (P. Panagiotopoulou).
0360-3199/$ – see front matter
doi:10.1016/j.ijhydene.2012.02.087

the concentration of CO should be reduced to less than 50 ppm, as dictated by the poisoning limit of Pt electrodes [1]. This is usually accomplished by treatment of the reformate gas in a WGS reactor, followed by a final purification step, which may involve preferential oxidation or methanation of residual CO [9–11].

Ethanol can be reformed at low temperatures (300–400 °C) toward a gaseous mixture containing H_2, CH_4 and carbon oxides. The CO content can be significantly reduced if a WGS activity function is included in the catalyst formulation. The elimination of CO from the reformate gas can also result in a decrease of CH_4 selectivity by retarding CO methanation, which may run in parallel in the temperature range of 300–400 °C, consuming significant quantities of hydrogen. The resulting gas mixture can then be used, without further treatment, to feed fuel cells for the production of electricity and heat.

Although the LTSR of ethanol has not been investigated extensively, catalysts based on Ni, Co, Cu, Ir, Pt, Rh, Pd and Ru dispersed on different supports (e.g., Al_2O_3, CeO_2, La_2O_3, ZrO_2, Y_2O_3, ZnO, Sm_2O_3, TiO_2, V_2O_5 and MgO) have been studied [7,12–25]. Generally, supported Pt catalysts seem to present higher activity and selectivity toward H_2 compared to other metals for the LTSR of ethanol and therefore are more widely studied [7,13]. It has been proposed that catalytic activity, selectivity and stability of Pt/CeO_2 catalysts increase with increasing Pt loading from 1 to 5 wt.% [14,17]. The best performing 5%Pt/CeO_2 catalyst is also active for the WGS reaction, resulting in the elimination of CO at the exit of the reformer [14]. The higher stability of Pt/CeO_2 compared to Pt/Al_2O_3 catalysts has been attributed to the ability of ceria to release and store oxygen [14].

The mechanism of ethanol steam reforming has been the subject of several studies. It has been proposed that dehydrogenation of molecularly adsorbed ethanol is the key reaction step over supported noble metal catalysts [26]. Ethylene (produced by dehydration of ethanol) was mainly formed on Al_2O_3-supported catalysts, whereas significant amounts of acetaldehyde (produced by dehydrogenation of ethanol) were also formed over CeO_2-supported catalysts [26]. Dömök et al. [27] found that different types of ethoxy species, traces of acetaldehyde as well as significant amounts of acetate groups were detected on the surface of Pt/Al_2O_3 catalyst. It has also been proposed that some reaction pathways are favored depending on the nature of the support, resulting in different product distribution in the gas phase [28]. For example, at low temperatures, acetate formation was enhanced over Pt/ZrO_2 catalyst, whereas the ethoxy decomposition to CO, CH_4 and H_2 was facilitated over Pt/CeO_2 catalyst [28].

In our previous study [7], the catalytic activity of Al_2O_3-supported noble metal catalysts for the reaction of steam reforming of ethanol was investigated in the temperature range of 300–450 °C. It was found that the catalytic performance varies in the order of Pt > Pd > Rh > Ru, with Pt exhibiting high activity and selectivity toward hydrogen production, as well as long term stability at low temperatures. In the present study, the catalytic performance of Pt catalysts for the title reaction is investigated with respect to the nature of the support (Al_2O_3, ZrO_2, CeO_2). The reaction mechanism is also studied over supported Pt catalysts, employing *in situ* FTIR and transient mass spectrometry (transient-MS) techniques. The aim is to identify the nature of active sites and adsorbed species involved in the steam reforming of ethanol and their relation with the gas phase products.

2. Experimental

2.1. Catalyst preparation and characterization

Catalysts were prepared employing the wet impregnation method [7] with the use of $(NH_3)_2Pt(NO_2)_2$ (Alfa) as metal precursor salt and the following commercial metal oxide powders as supports: γ-Al_2O_3 (Alfa products), CeO_2 (Alfa products), ZrO_2 (Alfa products). The nominal metal loading of catalysts thus prepared was 0.5 wt.%.

Carriers and catalysts were characterized with respect to their specific surface area, exposed metallic surface area and mean crystallite size employing nitrogen physisorption at liquid nitrogen temperature and selective chemisorption of H_2 (CO for Pt/CeO_2), at 25 °C. Details on the equipment and procedures used for catalyst characterization can be found elsewhere [9].

2.2. Apparatus and experimental procedures

2.2.1. In situ FTIR spectroscopy

Fourier transform infrared (FTIR) experiments were carried out using a Nicolet 6700 FTIR spectrometer equipped with a diffuse reflectance (DRIFT) cell (Spectra Tech), an MCT detector and a KBr beam splitter. The gas inlet of the cell was directly connected to a flow system, equipped with mass-flow controllers, saturators with ethanol and water, and a set of valves which allowed selection and control of feed gas composition. In a typical experiment, the catalyst powder was heated at 450 °C under He flow for 10 min and then reduced in flowing hydrogen (20%H_2 in He) at 300 °C for 60 min. The cell was then flushed with He at 450 °C for 10 min and subsequently cooled to room temperature (RT) under He flow. During the cooling stage, background spectra were collected at temperatures of interest. The flow was then switched to a gas mixture consisting of 0.5%CH_3CH_2OH+1.5% H_2O (in He) at RT for 30 min. Temperature was then increased in a stepwise mode up to 450 °C and spectra were obtained at selected temperatures after equilibration for 15 min-on-stream. After recording the spectrum, temperature was increased to the next selected temperature. In all experiments, the total flow through the DRIFT cell was 30 $cm^3\ min^{-1}$.

2.2.2. Transient experiments

Temperature-programmed surface reaction (TPSR) experiments were carried out using the apparatus and following the procedures which have been described in detail elsewhere [7]. In a typical TPSR experiment, 100 mg of the catalyst were placed in a quartz microreactor and reduced *in situ* at 300 °C under H_2 flow (30 $cm^3\ min^{-1}$) for 30 min. The sample was then heated under He flow (30 $cm^3\ min^{-1}$) at 500 °C for 15 min to remove adsorbed species from the catalyst surface and subsequently cooled to room temperature. At this point the feed composition was switched to a mixture containing 0.5%

CH_3CH_2OH+1.5% H_2O (in He) (30 cm^3 min^{-1}), by controlling the flow of three independent He lines, two of which passed through saturators containing ethanol and water. The catalyst was kept at room temperature for the first 5 min and temperature was then increased linearly ($\beta = 15$ °C/min) up to 750 °C. Immediately after the experiment, the catalyst was cooled to room temperature under He flow and the feed composition was switched to 3%O_2 (in He) (30 cm^3 min^{-1}). After 10 min of exposure at room temperature, the catalyst was heated linearly ($\beta = 30$ °C/min) up to 750 °C under O_2 flow (Temperature-Programmed Oxidation, TPO).

An Omnistar/Pfeiffer Vacuum mass spectrometer (MS) was used for on-line monitoring of effluent gas composition. The transient-MS signals at $m/z = 2$ (H_2), 15 (CH_4), 18 (H_2O), 28 (CO), 44 (CO_2), 31 (C_2H_5OH), 29 (C_2H_4O), 26 (C_2H_4), 27 (C_2H_6), 39 (C_3H_6) and 59 ($C_4H_{10}O$) were continuously recorded. Responses of the mass spectrometer were calibrated against standard mixtures of accurately known composition. Fragmentation of the different species was calibrated and contributions from other than the indicated ones were subtracted, as well as the backround level". When necessary (e.g. CO_2-CO signals), the cracking coefficient determined in separate experiments was also taken into account in the calculations of gas effluent concentrations. For example, to compensate for the contributions from CO_2 to $m/z = 28$, the $0.2 \cdot (m/z = 44)$ was subtracted from $m/z = 28$ to obtain the signal representing CO.

2.2.3. Catalytic performance tests under steady-state conditions

Catalytic performance tests were carried out using an apparatus which has been described in detail elsewhere [7]. Briefly, it consists of a flow measuring and control system equipped with four mass-flow controllers (MKS), an HPLC pump (Marathon Scientific Systems) and an evaporator for feeding the ethanol/water stream, a quartz microreactor and two gas chromatographs (Shimadzu), connected in parallel through a common set of switch valves, for on-line analysis of reactants and products. The first GC is equipped with two packed columns (Porapak-Q, Carbosieve) and two detectors (TCD, FID) and operates with He as the carrier gas. The second GC is equipped with a Carbosieve column and a TCD detector. This chromatograph uses N_2 as the carrier gas and was solely used for the determination of H_2 in the reformate gas.

The catalytic performance of the prepared samples for the steam reforming of ethanol has been investigated in the temperature range of 300–400 °C using a feed stream consisting of 12.5%CH_3CH_2OH+37.5%H_2O (He balance). In a typical experiment, 650 mg of fresh catalyst ($0.18 < d < 0.25$ mm) is placed in the reactor and reduced *in situ* at 300 °C for 2 h under a hydrogen flow of 60 cm^3 min^{-1}. After purging with He for 15 min the sample was exposed to the reaction mixture (120 cm^3 min^{-1}), and ethanol conversion as well as product distribution were determined as a function of reaction temperature. All experiments were performed at near atmospheric pressure.

3. Results and discussion

3.1. Catalyst characterization

Specific surface areas (SSA) of commercial metal oxide supports used in the present study were measured with the BET method and results are reported in Table 1 along with Pt dispersion and mean crystallite size (d_{Pt}) of synthesized catalysts. It is observed that the metal dispersion and mean crystallite size vary between 65.1 and 99% and 0.7–1.6 nm, respectively.

3.2. Influence of the nature of the support on catalytic performance

The possible occurrence of homogeneous reactions has been investigated in a previous study over a bed of quartz particles in the temperature range of 300–650 °C. It was found that, within the temperature range of interest (<450 °C), no homogeneous reactions take place, under the present experimental conditions [7].

The effect of the nature of the support on catalytic performance was investigated over Pt catalysts of the same metal content (0.5 wt.%) supported on three commercial metal oxide powders (Al_2O_3, CeO_2, ZrO_2). Results obtained are summarized in Fig. 1A, where the conversion of ethanol is shown as a function of reaction temperature. It is observed that the Pt/ZrO_2 catalyst exhibits a superior performance compared to Pt/CeO_2, whereas Pt/Al_2O_3 exhibit intermediate performance. Conversion of ethanol increases with increasing temperature and reaches 100% at ca 360 °C for Pt/ZrO_2 and Pt/Al_2O_3 catalysts, while temperatures higher than 380 °C are required, for CeO_2-supported catalyst, in order to achieve conversions above 90%.

Product distribution obtained over the Pt/CeO_2 catalyst is shown in Fig. 1B as a function of reaction temperature. It is observed that the main products detected are H_2, CH_4, CO, CO_2, CH_3CHO and, to a smaller extent C_2H_6 and C_2H_4. Selectivity toward hydrogen production increases from 37 to 44%, with increasing temperature from 300 to 400 °C. Hydrogen selectivity is defined as the concentration of gas phase hydrogen at reactor effluent over the concentration of all products containing hydrogen, multiplied with the proper factor (e.g. for CH_4 is 2). Selectivity toward methane is also high, varying between 39 and 47% in the temperature range

Table 1 – Physicochemical characteristics of the synthesized catalysts.

Catalyst	Specific surface area (SSA) (m^2/g)	Metal dispersion (%)	Metal crystallite size (nm)
0.5%Pt/Al_2O_3	83.0	99.0	0.7
0.5%Pt/CeO_2	3.3	93.3	1.1
0.5%Pt/ZrO_2	51.0	65.1	1.6

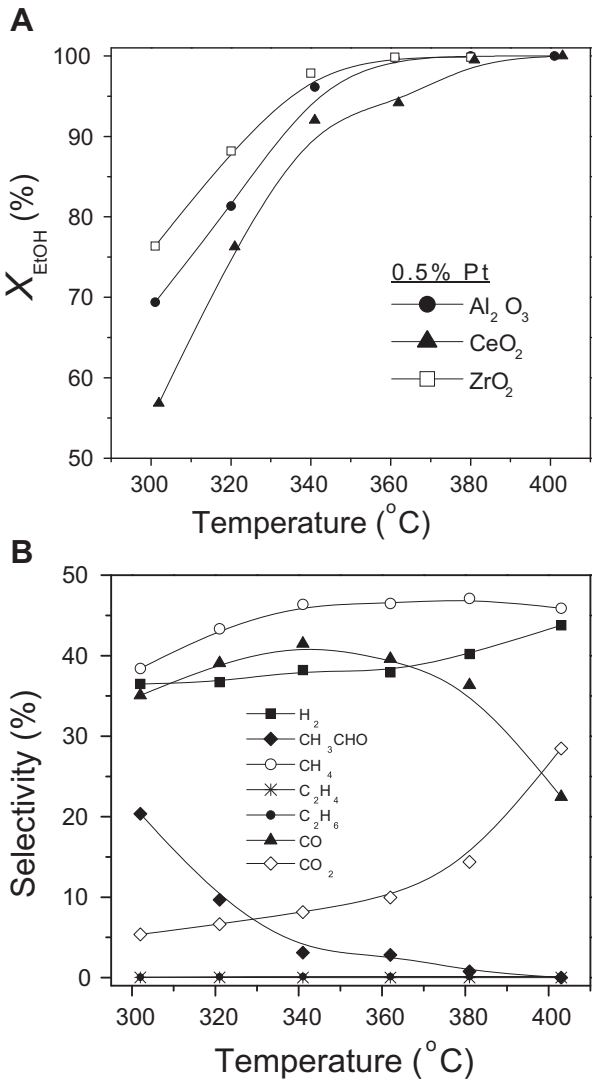

Fig. 1 – (A) Effect of the nature of the support on the catalytic performance over Pt (0.5 wt.%) supported on the indicated commercial oxide carriers. (B) Selectivity toward reaction products as a function of reaction temperature over 0.5% Pt/CeO_2 Experimental conditions: Mass of catalyst: 0.65 g; particle diameter: 0.18 < d_p < 0.25 mm; Total Flow: 120 cm^3/min; GHSV = 9350 h^{-1}; Feed composition: 12.5% EtOH, 37.5% H_2O (balance He); P = 1atm.

examined. At low temperatures, carbon monoxide selectivity is comparable to that of H_2, while above 360 °C it decreases substantially, reaching 23% at 400 °C. Inverse behavior to that of CO is observed for the variation of CO_2 selectivity, which increases from 6 to 29% in the temperature range of 300–400 °C. Results imply that production of CO_2 takes place at the expense of CO, due to the occurrence of the WGS reaction. This is in agreement with previous studies [9,11] over Pt supported catalysts, where it has been reported that the WGS reaction (Eq. (2)) occurs with high rates at temperatures above 350 °C.

$$CO + H_2O \rightarrow CO_2 + H_2 \quad \Delta H^o_{298} = -41.1 \text{ kJ mol}^{-1} \tag{2}$$

The production of H_2, CH_4 and CO may be attributed to ethanol decomposition (3), which can occur either directly (Eq. (3)) or via intermediate formation of acetaldehyde as a sum of reactions (4) and (5):

$$C_2H_5OH \rightarrow CH_4 + H_2 + CO \quad \Delta H^o_{298} = 49.4 \text{ kJ mol}^{-1} \tag{3}$$

$$C_2H_5OH \rightarrow CH_3CHO + H_2 \quad \Delta H^o_{298} = 68.5 \text{ kJ mol}^{-1} \tag{4}$$

$$CH_3CHO \rightarrow CH_4 + CO \quad \Delta H^o_{298} = -19 \text{ kJ/mol} \tag{5}$$

The latter pathway is supported by the high selectivity toward CH_3CHO at temperatures lower than 360 °C (S_{CH_3CHO} = 3–21%) observed in Fig. 1B. Traces of ethylene were also detected in the gas phase, the production of which may take place via the dehydration reaction (Eq. (6)) [13,26].

$$C_2H_5OH \rightarrow C_2H_4 + H_2O \quad \Delta H^o_{298} = -45.3 \text{ kJ mol}^{-1} \tag{6}$$

However, the low concentration of ethylene ($S_{C_2H_4} < 0.03\%$), indicates that either dehydration reaction is not promoted over the Pt/CeO_2 catalyst, or that this molecule is transformed rapidly on the catalyst surface. The latter explanation is more probable and is supported by the fact that higher amounts of ethane (compared to ethylene) are present at high temperatures ($S_{C_2H_6} \sim 0.14\%$), probably due to the hydrogenation of ethylene.

The product distribution over Pt catalysts supported on Al_2O_3 and ZrO_2 (not shown) is qualitatively similar to that discussed above for 0.5% Pt/CeO_2 catalyst (Fig. 1B). Hydrogen selectivity takes values between 35 and 47% for all catalysts investigated and is higher, at a given temperature, over Pt/ZrO_2 and Pt/Al_2O_3 compared to Pt/CeO_2 catalyst. Different is the ranking of metal oxide supports with respect of methane selectivity, which was found to vary between 37 and 47% at 320 °C, in the order of $Al_2O_3 > CeO_2 > ZrO_2$. The nature of the metal oxide support also affects the production of acetaldehyde via dehydrogenation reaction (Eq. (4)). In particular, S_{CH_3CHO} decreases from 14 to 6% at 320 °C following the order $ZrO_2 > CeO_2 > Al_2O_3$.

It is of interest to note that the main difference observed between the investigated supports is related to the variations of CO and CO_2 selectivities. As discussed above, carbon dioxide concentration increases with increasing temperature at the expense of carbon monoxide, due to the occurrence of the WGS reaction (Eq. (2)). It has been found in previous studies that the WGS activity of dispersed platinum depends strongly on the physicochemical characteristics of the support, and is about 1–2 orders of magnitude higher when supported on "reducible" compared to "irreducible" metal oxides [11,29,30]. In Fig. 2, selectivity toward CO for the low temperature steam reforming of ethanol over the investigated catalysts is presented as a function of temperature. It is observed that S_{CO} is significantly affected by the nature of the support, following the order $CeO_2 > Al_2O_3 > ZrO_2$. This order is rather unexpected since CeO_2 is characterized by higher reducibility compared to Al_2O_3 and it has been previously found that Pt/CeO_2 catalyst is sufficiently active for the WGS reaction [29,31–33]. However, the investigated CeO_2 carrier is characterized by low specific surface area (3.3 m^2/g), which is

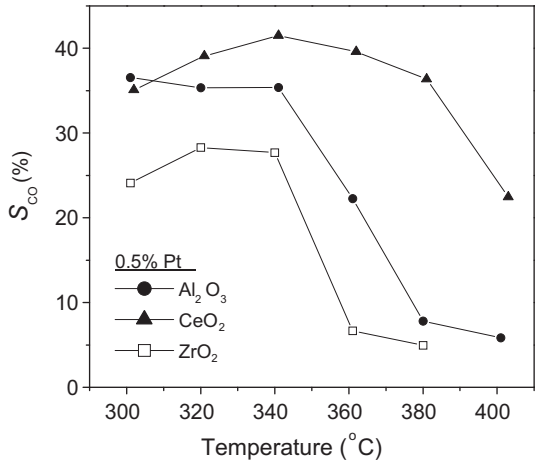

Fig. 2 – Effect of the nature of the support on the selectivity toward CO over Pt (0.5 wt.%) supported on the indicated commercial oxide carriers. Experimental conditions: same as in Fig. 1.

well known to affect the reducibility and consequently, the WGS activity [9,34]. In particular, in our previous study [34] it has been found that the reducibility of titania support increases with increasing the specific surface area of the catalyst. It has been also reported that the WGS activity increases with increasing the reducibility of TiO_2. Regarding the low temperature steam reforming of ethanol, experiments have been conducted over Pt catalyst dispersed on ZrO_2 support of lower SSA (4 m^2/g) compared to that of ZrO_2 support (51 m^2/g) used in the present study. Results (not presented) showed that although, ethanol conversion is not affected significantly by the SSA of ZrO_2, selectivity toward CO decreases substantially with increasing the SSA of ZrO_2 support. This was accompanied by a parallel increase of CO_2 selectivity, indicating the enhancement of the WGS activity. Although, no similar experiments were conducted for Pt supported on CeO_2 carriers, the above results provide evidence that the higher selectivity toward CO observed for the Pt/CeO_2 catalyst can be attributed to the inhibition of the WGS reaction due to its low SSA.

Different rankings of metal oxide supports, with respect to their activity for the low temperature steam reforming of ethanol, have been reported in the literature. For example, Llorca et al. [20] found that optimum results were obtained over ZnO-, La_2O_3-, Sm_2O_3- and CeO_2-supported Co catalysts, which resulted in the production of a CO-free hydrogen gas stream. The beneficial effect of CeO_2 support for the low temperature steam reforming of ethanol has also been reported by Ciambelli et al. [31] who found that hydrogen yield is higher and more stable for Pt/CeO_2 than for Pt/Al_2O_3 catalysts. Product distribution was also found to be influenced by the nature of the support, with Pt/CeO_2 catalyst exhibiting higher selectivities toward H_2 and CO_2 and lower selectivity toward CO, due to the enhancement of the WGS reaction. The differences between the latter results and those shown in Figs. 1 and 2 may be attributed to the different specific surface area of the ceria support used, which was significantly higher (80 m^2/g) compared to that of CeO_2 sample (3 m^2/g) used in the present study.

3.3. Investigation of the reaction mechanism

3.3.1. *In situ* FTIR spectra

Mechanistic aspects of the ethanol steam reforming reaction have been investigated with the use of transient-MS and FTIR techniques. The *in situ* DRIFT spectra obtained following exposure of the Pt/Al_2O_3 catalyst to a flowing 0.5% EtOH+1.5% H_2O (balance He) mixture at 25 °C for 30 min and subsequent stepwise heating at 450 °C are shown in Fig. 3A. It is observed that the spectrum recorded at 25 °C (trace a) is characterized by negative bands in the ν(OH) region (3850–3400 cm^{-1}) as well as by several bands in the C-H stretching frequency region (3100–2700 cm^{-1}) and in the C-H deformation and C-O stretching regions (1600–950 cm^{-1}). The two negative bands located at 3750 and 3685 cm^{-1} can be attributed to losses of ν(OH) intensity of (at least) two different types of free hydroxyl groups initially present on the Al_2O_3 surface [35], the population of which decreased following interaction with ethanol at room temperature. It is well known that free hydroxyl groups of Al_2O_3 can hydrogen-bond to adsorbed ethanol and ethoxy (CH_3O-) species, thereby resulting in a loss of intensity for free OH species [13,27]. Raskó et al. [13] reported that ethanol can adsorb in two molecular forms on the catalyst surface: in an adsorbed form coordinated to Lewis acid sites of the support and in a hydrogen-bridge bonded form through the OH groups of supporting oxides. Based on literature results [13,27,36], the bands detected at ca.1450 cm^{-1} ($\delta(CH_3)$ in ethanol), 1386 cm^{-1} ($\delta(CH_3)$ in ethanol) and 1278 cm^{-1} (δ(OH) in ethanol), can be attributed to ethanol molecularly adsorbed on the Al_2O_3 surface.

Regarding the peaks in the ν(C-H) region, located at 2975, 2933 and 2896 cm^{-1} (trace a), they can be assigned to C-H stretching vibrations in methyl groups ($CH_{3,ad}$) and to symmetric and asymmetric C-H vibrations in methylene groups ($CH_{2,ad}$), respectively [13,27].

The band located at 1650 cm^{-1} is due to carbonate and/or bicarbonate species [13,27,36], and those at 1577 cm^{-1} to formate species associated with the Al_2O_3 support [36]. The weak peak located at ca 1108 cm^{-1} can be attributed to ethoxide coordinated to a single surface cation of the support (monodentate ethoxide) [13].

Stepwise increase of temperature from 25 to 450 °C results in the progressive development of a broad band located at around 2028 cm^{-1} at 100 °C (traces b), which indicates the presence of adsorbed CO species on the Pt surface. At temperatures higher than 100 °C two peaks can be distinguished in this frequency region, located at ca 2063 (shoulder) and 2033 cm^{-1}, which can be attributed to CO linearly adsorbed on partially oxidized ($Pt^{\delta+}$) [34,37,38] and reduced (Pt^0) platinum sites [39,40], respectively. However, as it will be discussed in detail below, similar bands are often assigned to CO linearly adsorbed on Pt terrace and step sites, respectively [39–41]. Increasing temperature results in a progressive shift of the peak maxima toward lower wavenumbers, which is consistent with a decrease in the dipole–dipole coupling effect between adsorbed CO molecules with decreasing coverage [34,37,38]. The intensity of this broad band exhibits

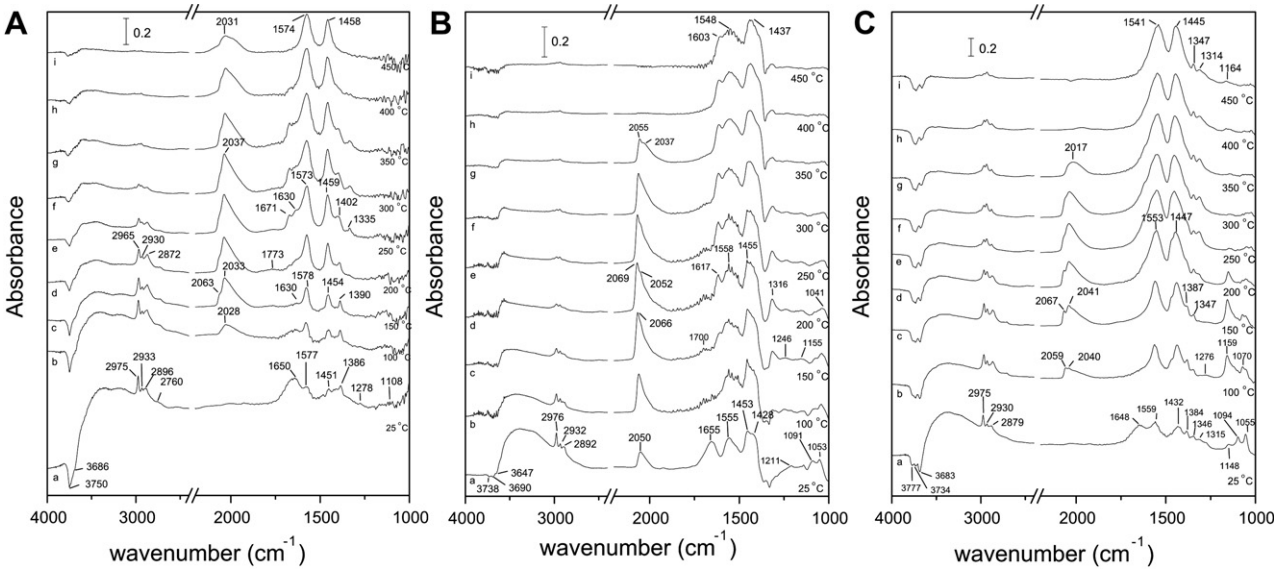

Fig. 3 – DRIFT spectra obtained over Pt catalysts supported on (A) Al_2O_3, (B) CeO_2 and (C) ZrO_2 following interaction with the reaction mixture 0.5% EtOH, 1.5% H_2O (He balance) at 25 °C for 30 min and subsequent stepwise heating at 450 °C.

a maximum at ca 300 °C (traces b–f) and decreases upon further increase of temperature to 450 °C (traces g–i). This is probably due to either CO desorption or to its participation in surface reactions. It is of interest to note that the development of the later band is taking place at the expense of bands at 2975, 2933 and 2896 cm^{-1} ($\nu(CH_3)$, $\nu(CH_2)$), which disappear above 300 °C. A new weak band is also detected at ca. 1773 cm^{-1} at temperatures higher than 100 °C, which is attributed to bridge bonded CO and disappears above 200 °C (traces c–e).

Regarding the bands below 1700 cm^{-1}, it is observed that those correspond to molecularly adsorbed ethanol decrease in intensity with increasing temperature. The population of formates (1577 cm^{-1}) progressively increases with increasing temperature, providing evidence that the produced CO interacts with the hydroxyl groups of the catalyst surface to yield formates. However, above 100 °C the band at ca. 1573 cm^{-1} may contain contribution from a new band, which is developed in parallel with that at ca. 1459 cm^{-1}. Both latter bands are present in the spectra detected up to 450 °C and can be attributed to the symmetric (1459 cm^{-1}) and asymmetric (1573 cm^{-1}) vibration of the O–C–O group in acetate species [27,36,42,43]. It should be noted that the two main bands in the region of 1700–1300 cm^{-1} are accompanied by several shoulders at temperatures higher than 200 °C, implying the presence of carbonate and/or bicarbonate species (1402, 1355 cm^{-1}) on the surface of Al_2O_3 support [36].

It is of interest to note that, above 150 °C, the progressive development of the bands due to acetate species (1573, 1459 cm^{-1}) is accompanied by the appearance of two new bands located at 1671 and 1630 cm^{-1}, the intensity of which goes through a maximum at around 250–300 °C and then decreases with further increasing temperature. Similar bands with that at 1630 cm^{-1} have been previously attributed to adsorbed crotonaldehyde, which can be formed by aldolization of two acetaldehyde molecules [13]. However, no evidence has been provided for the presence of crotonaldehyde in the catalytic performance tests under steady-state or, as it will be discussed below, under transient conditions. Regarding the shoulder at 1671 cm^{-1}, it can be assigned to ν(C=O) of adsorbed acetaldehyde, as acyl species, originating from ethanol dehydrogenation reaction (Eq. (4)), on the surface of Al_2O_3 [13,27]. It has been proposed that the produced acetaldehyde can be oxidized by OH groups over the alumina surface resulting in the formation of surface acetates species (Eq. (7)) or it can decomposed to methane and carbon monoxide (Eq. (8)) [27,36]:

$$CH_3CHO_{(ad)} + OH \rightarrow CH_3COO_{(ad)} + H_2 \quad (7)$$

$$CH_3CHO_{(ad)} \rightarrow CH_4 + CO_{(ad)} \quad (8)$$

Dömök et al. [27] proposed that acetate species can be decomposed toward $CH_{3(ad)}$ species (Eq. (9)), which can be further react with surface OH groups producing carbon monoxide (Eq. (10)).

$$CH_3COO_{(ad)} \rightarrow CH_{3(ad)} + CO_2 \quad (9)$$

$$CH_{3(ad)} + OH_{(ad)} \rightarrow CO + 2H_2 \quad (10)$$

This may be the case for the results of the present study, since, as discussed above, the consumption of $CH_{x(ad)}$ species corresponding to the bands at 2975, 2933 and 2896 cm^{-1} is accompanied by the development of the band assigned to CO linearly adsorbed on Pt crystallites.

Similar FTIR spectra were obtained for Pt/CeO_2 catalyst and results obtained are shown in Fig. 3B. It is observed that at room temperature the spectrum is dominated by bands corresponding to different vibrational modes of ethoxy species, which were formed by dissociative adsorption of ethanol over

Ce cations (2976, 2932, 2892 cm^{-1}: ν(CH), 1428 cm^{-1}: $\delta_{as}(CH_3)$, 1053, 1091 cm^{-1}: ν(CO)) [44,45], acetate species (1453 cm^{-1}: ν_s(OCO), 1555 cm^{-1}: ν_{as}(OCO)) [13,44,45] and linearly adsorbed CO species (2050 cm^{-1}: CO-Pt^0) [38,44]. The band at 1211 cm^{-1} is probably due to molecularly adsorbed ethanol [45], whereas that at 1655 cm^{-1} can be attributed to carbonate species associated with the support [38,44]. Apart from the carbonyl bands discussed above, interaction of the reaction mixture with the Pt/CeO_2 catalyst results in the development of three negative bands located at 3738, 3690 and 3647 cm^{-1} (Fig. 3B), which characterize OH stretching modes of three types of different surface hydroxyl groups [46].

Stepwise increase of temperature up to 250 °C results in the progressive increase of the relative intensity of the band corresponding to linearly adsorbed CO, which starts to decrease with further increasing temperature and disappears above 400 °C. As in the case of Pt/Al_2O_3 catalyst, two bands are discernible in this frequency region, located at ca 2069 and 2052 cm^{-1}, in the temperature range of 200–350 °C (traces d–g).

It is worth noticing that two new weak bands appear at ca 1700 and 1155 cm^{-1} in the temperature range of 100–300 °C (traces b–f), which have been previously assigned to adsorbed acetaldehyde species [13,44,45,47,48]. At temperatures higher than 100 °C two new bands are detected at 1617 and 1316 cm^{-1}, which are present in the spectra obtained up to 450 °C and can be assigned to the ν(CO) vibrational mode of acetyl species [45,49] and to carbonate species [43], respectively. It seems that the formation of acetyl and acetate species is taking place at the expense of ethoxy and acetaldehyde species, which disappear above 350 °C.

DRIFTS spectra obtained from the Pt/ZrO_2 catalyst are shown in Fig. 3C. It is observed that interaction of the catalyst with the reformate mixture at room temperature results in the appearance of bands due to different vibrational modes of ethoxy (1094, 1055, 1384, 2975, 2930 and 2879 cm^{-1}) [28,50], acetate (1559, 1432, 1346 and 1315 cm^{-1}) and acetyl species (1648 cm^{-1}) [28,50], as well as by negative bands (3777, 3734 and 3683 cm^{-1}) related to the consumption of surface OH groups during the interaction of ethanol with the catalyst surface. Increase of temperature to 100 °C results in the development of a broad band in the ν(CO) frequency region (2100–2000 cm^{-1}), which is characterized by two maxima at ca 2059 and 2040 cm^{-1} attributable, as discussed above, to linearly adsorbed CO species.

As in the case of Pt/Al_2O_3 (Fig. 3A) and Pt/CeO_2 (Fig. 3B) catalysts, the population of acetate species increases with increasing temperature at the expense of ethoxy species, probably due to dehydrogenation of the latter species toward acetaldehyde. Acetaldehyde can be further dehydrogenated to acetyl species, which, in turn, can be decomposed toward CH_4 and adsorbed CO species ((Eq. (8)). Comparison of the results of Fig. 3A, B and C shows that the formation of acetate species takes place at lower temperatures over Pt/CeO_2 and Pt/ZrO_2 catalysts, indicating that the dehydrogenation of ethoxy species is enhanced on the surface of these catalysts. The presence of acetate species even at room temperature over CeO_2-supported catalysts has been previously attributed to the large availability of oxygen from the ceria support [45]. It should be noted that in the case of Pt/ZrO_2 catalyst, the band corresponding to acetyl species (1648 cm^{-1}) is discernible only in the spectra obtained at room temperature, whereas in the case of Pt/CeO_2 (1617 cm^{-1}) and Pt/Al_2O_3 (1671 cm^{-1}) catalysts, it can be discerned up to 450 °C. This provides evidence that decomposition of acetyl species is favored over Pt/ZrO_2 catalyst and, as it will be discussed below, it can be correlated with the higher activity and selectivity of this catalyst toward hydrogen.

Comparison of the DRIFTS spectra obtained from Pt/Al_2O_3 (Fig. 3A), Pt/CeO_2 (Fig. 3B) and Pt/ZrO_2 (Fig. 3C) catalysts, shows that the nature of the support affects significantly the relative intensity of the two bands detected in the ν(CO) frequency region located at ca 2063–2070 cm^{-1} and 2035–2055 cm^{-1}. This is clearly shown in Fig. 4, where the DRIFT spectra obtained from all catalysts investigated at 150 and 200 °C, are

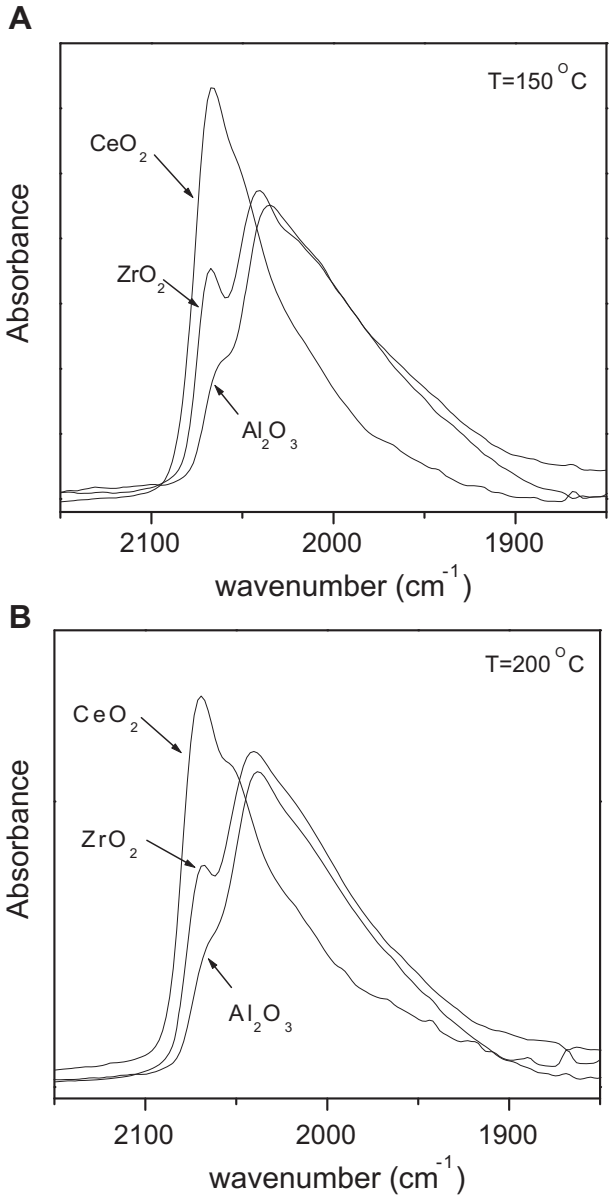

Fig. 4 – DRIFT spectra obtained at 150 °C and 200 °C from Pt catalysts supported on Al_2O_3, CeO_2 and ZrO_2 under conditions similar to those of Fig. 3.

presented. It is observed that the ratio of the Low Frequency (LF) to High Frequency (HF) band intensity follows the order $Al_2O_3 > ZrO_2 > CeO_2$ which is more or less similar to the catalytic activity order presented in Fig. 1A. As discussed previously, these bands can be assigned to CO linearly adsorbed either on partially oxidized ($Pt^{\delta+}$) [34,37,38] and reduced (Pt^0) platinum sites [39,40], respectively, or on Pt terrace and step sites, respectively [39–41]. Liu et al. [41] reported that the ratio of terrace to step sites on the surface of Pt increases with increasing platinum crystallite size. However, this is not the case here since the relative intensities of the LF and HF bands do not follow any trend related to Pt crystallite size (Table 1). Therefore, the bands at ca 2063–2070 cm^{-1} and 2035–2055 cm^{-1} can be assigned to CO linearly adsorbed on partially oxidized ($Pt^{\delta+}$) and reduced (Pt^0) platinum sites, respectively. Dömök et al. [27] reported that at low temperatures the catalyst surface is modified during the reaction, resulting in poisoning of Pt sites. They proposed that either Pt is oxidized during the reaction or a surface species is formed which hinders the process. Oxidation of Pt sites is possible to take place in the present study, since the relative intensity of the band attributable to $Pt^{\delta+}$ sites increases with increasing temperature in the case of the less active Pt/CeO_2 (Fig. 3B) catalyst, and decreases with increasing the efficiency of the support (Fig. 4). Furthermore, it is obvious that, although Pt/CeO_2 catalyst is initially active to transform ethoxy species to acetate even at room temperature, which can be then decomposed to adsorbed CO species, its activity is decreased probably due to oxidation of platinum surface.

Erdohelyi et al. [26] reported that acetate species, which are located primarily on the support, can poison the catalyst. They suggested that highly stable acetate species hinder the migration of ethoxide species to the metal, and consequently, the decomposition of the latter species at the metal/support interface toward H_2 formation. Although no such evidence can be provided from the results of Fig. 3, it is possible that accumulation of acetate species on the catalyst surface is responsible for the differences observed in catalytic activity and selectivity to H_2 over supported Pt catalysts.

It should be noted that the LF-linear CO band observed at ca. 2056 cm^{-1} at 200 °C for Pt/CeO_2 catalyst appears at lower wavenumbers (2038–2040 cm^{-1}) for Pt/Al_2O_3 and Pt/ZrO_2 catalysts (Fig. 4), indicating that the adsorption strength of the carbon-oxygen (C-O) bond is weaker over the latter catalysts. This can be attributed to metal–support interactions which affect the chemisorption properties of Pt and may results in the formation of Pt carbonyl hydrides [50].

It is worth to notice that adsorbed CO species disappear from the spectra at lower temperatures (>350 °C) over Pt/ZrO_2 and Pt/CeO_2 catalysts compared to Pt/Al_2O_3 catalyst where it can be discerned up to 450 °C (Fig. 3). This can be correlated with the high activity of these catalysts for the WGS reaction, which has been proposed to proceed via interaction of adsorbed CO with surface hydroxyl groups to form intermediate formate species, which is further decomposed toward CO_2 and H_2 [9,34,46]. Dömök et al. [50] suggested that the WGS reaction over Pt/ZrO_2 catalyst is taking place via decomposition of acetate groups at the metal/support interface and interaction of the so formed products with the OH groups activated on the partially reduced zirconia sites. The detection of adsorbed CO and acetate species up to 450 °C over Pt/Al_2O_3 catalyst indicates that the formation rate of these species is higher than their decomposition or further reaction.

3.3.2. *Transient-MS results*

The reaction scheme of steam reforming of ethanol as a function of temperature was investigated employing transient experiments over Pt (0.5 wt.%) catalysts supported on Al_2O_3, CeO_2 and ZrO_2. The experiments were conducted using an ethanol-water mixture of molar ratio $EtOH:H_2O = 1:3$ (0.5% EtOH, 1.5% H_2O, balance He) and a linear temperature ramp of 15 °C/min, from 25 to 750 °C. The reactor effluent was continuously monitored by mass spectrometer, as described in the experimental section. TPSR profiles obtained from the $0.5\%Pt/Al_2O_3$ catalyst are shown in Fig. 5A. It is observed that ethanol is adsorbed onto the catalyst surface at low temperatures, until the surface is saturated, and it appears in the gas phase between 80 and 300 °C. Ethanol decomposition and dehydrogenation reactions (Eq.(3),(4)), are initiated in the same temperature range producing H_2, CO, CH_4 and CH_3CHO. The concentrations of CO and CH_4 are similar, as expected from Eq. (3), in contrast to H_2 concentration which is significantly higher. This may be due to the occurrence of reaction (4) and, simultaneously, ethanol dehydration reaction (Eq. (6)), followed by decomposition of the produced ethylene (Eq. (11)) toward carbon and hydrogen:

$$C_2H_4 \rightarrow 2C + 2H_2 \quad (11)$$

Another possible route for further hydrogen production is via decomposition of CH_x species, which have been observed to adsorb on the catalyst surface (Fig. 3A), eluting hydrogen (Eq. (10)).

The decrease in the concentration of CO, at about 280–450 °C, which is accompanied by increase of the CO_2 peak and a slight increase of H_2 concentration, are attributed to the WGS reaction (Eq. (2)), which is known to occur in this temperature range over Pt catalysts [9,11,29,30]. However, the significant difference between the concentrations of H_2 and CO_2 provides evidence that the WGS reaction is not the only reaction taking place. The detection of traces of acetaldehyde, in association with the increasing CO and CH_4 concentrations up to 450 °C, indicates that acetaldehyde (Eq. (5)) or ethanol (Eq. (3)) decomposition reactions may also take place. According to the latter reaction, CO and CH_4 should follow identical patterns, but CH_4 concentration is higher than CO. In addition to CO consumption via the WGS reaction, this may be due to the methanation reaction [7,51]:

$$CO + 3H_2 \rightarrow CH_4 + H_2O \quad \Delta H^o_{298} = -206.2 \text{ kJ mol}^{-1} \quad (12)$$

In the temperature range of 450–550 °C, the increase of H_2 and CO concentrations, in association with the decreasing CO_2 and CH_4 concentrations, indicate that the dry methane reforming (Eq. (13)) is the main reaction taking place, which is completed at about 600 °C, as evidenced by the substantial decrease of methane concentration.

$$CH_4 + CO_2 \rightarrow 2CO + 2H_2 \quad \Delta H^o_{298} = 247 \text{ kJ mol}^{-1} \quad (13)$$

The CO_2 formation rate continues to decrease above 600 °C, probably due to the reverse WGS reaction. At temperatures

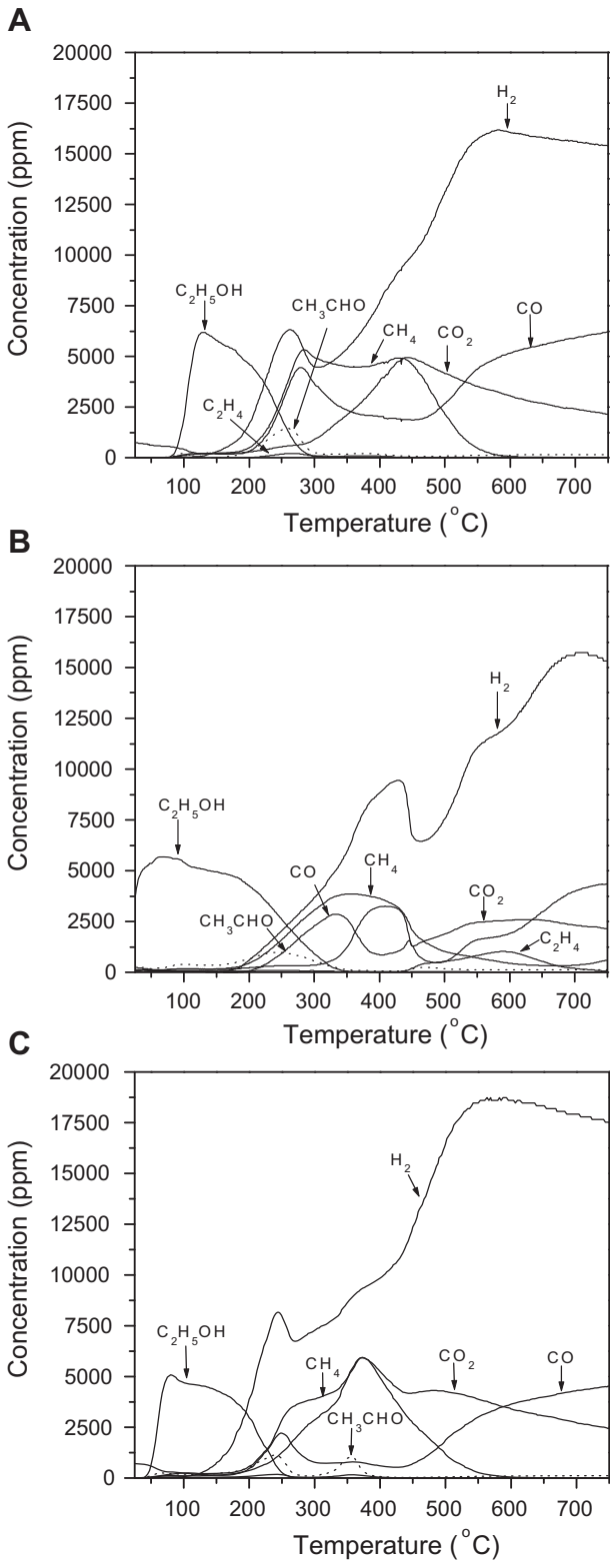

Fig. 5 – Spectra of temperature-programmed reaction under steam reforming conditions over Pt catalysts supported on (A) Al_2O_3, (B) CeO_2 and (C) ZrO_2. Experimental conditions: Mass of catalyst: 100 mg; particle diameter: $0.18 < d_p < 0.25$ mm; Total Flow: 30 cm^3/min; Feed composition: 0.5% EtOH, 1.5% H_2O (He balance); $\beta = 15$ °C/min; $P = 1$atm.

above 600 °C, steam reforming of ethanol (Eq. (14)) dominates, leading to high CO and H_2 concentrations:

$$C_2H_5OH + 2H_2O \rightarrow 2CO + 4H_2 \quad \Delta H^o_{298} = 497.5\ kJ/mol \qquad (14)$$

Results of a similar TPSR experiment conducted over the 0.5% Pt/CeO_2 catalyst are shown in Fig. 5B. It is observed that a part of ethanol is adsorbed onto the catalyst surface at room temperature (during the first 5 min), until the surface is saturated, and it elutes between 25 and 350 °C. Two more processes seem to compete, in the temperature range of 150–300 °C, namely decomposition of adsorbed ethanol (Eq. (3)) toward CO, H_2 and CH_4 and, to a smaller extent, ethanol dehydrogenation (Eq. (4)) producing acetaldehyde [51]. This is in accordance with the DRIFT spectra of Fig. 3B, where bands attributed to adsorbed acetaldehyde species appears in the narrow temperature range of 150–300 °C. Traces of C_2H_4 are also detected in the temperature range of 100–350 °C providing evidence that ethanol dehydration (Eq. (6)) takes place to a small extend. The concentrations of H_2 and CH_4 are similar, as expected from Eq. (3), in contrast to CO concentration which is slightly lower. This may be due to the parallel occurrence of the WGS reaction (Eq. (2)), as evidenced by the small increase of CO_2 concentration between 200 and 300 °C. The substantial decrease in the concentration of CO above 320 °C, which is accompanied by increase of the CO_2 and H_2 concentrations, indicates that the latter reaction is greatly enhanced at about 320–400 °C over Pt/CeO_2 catalyst [9,11,29,30]. However, as in the case of Pt/Al_2O_3 catalyst, H_2 concentration is significantly higher compared to that of CO_2, indicating the occurrence of parallel reactions in the same temperature range. The detection of CH_4, in association with increasing CO concentration up to 450 °C, indicates that ethanol (Eq. (3)) decomposition reaction may also take place. The decrease of H_2 concentration between 430 and 470 °C, which is accompanied by a decrease in CO concentration, may be due to the methanation reaction [7,51].

At temperatures higher than 500 °C, the concentrations of H_2 and CO increases again, accompanied by a decrease of CH_4 concentration, indicating that the methane steam reforming reaction (Eq. (15)) is taking place.

$$CH_4 + H_2O \rightarrow CO + 3H_2 \quad \Delta H^o_{298} = 206.2\ kJ\ mol^{-1} \qquad (15)$$

Above 550 °C, H_2 and CO concentrations continue to increase, before they become nearly steady at about 600 °C, where methane reforming is almost completed. The detection of ethylene in the temperature range of 450–700 °C provides evidence that the dehydration reaction (Eq. (6)) is taking place. At temperatures above 600 °C, steam reforming of ethanol (Eq. (14)) dominates, leading to high CO and H_2 concentrations.

The increase of CO_2 concentration above 550 °C can be related to the formation of acetate species, which, as it was shown in Fig. 3B, are present on the catalyst surface even at high temperatures. It is possible that acetate species can be oxidized toward carbonate species, which, in turn, are decomposed to CO_2 (Eq. (9)) [45]. Erdőhelyi et al. [26] proposed that acetate species formed on the metal oxide support migrate to the vicinity of the metal particles at high temperatures, where decompose to CO_2 (reverse spillover).

A similar TPSR experiment was conducted over the Pt/ZrO_2 catalyst and results obtained are presented in Fig. 5C. The ethanol peak is still present at low temperatures but it is now much smaller, indicating the higher reactivity of this material, even at temperatures as low as 150 °C. Ethanol is detected in the gas phase between 40 and 270 °C, with the parallel onset of decomposition and dehydrogenation reactions (Eq. (3),(4)), which are the dominant reactions in the temperature range of 200–300 °C, producing hydrogen. The concentrations of CO and CH_4 are similar up to 250 °C, as expected from the stoichiometry of Eq. (3). However, H_2 concentration is significantly higher, probably due to the occurrence of reaction (4) and, simultaneously, ethanol dehydration reaction (Eq. (6)), followed by decomposition of the produced ethylene toward carbon and hydrogen (Eq. (11)). However, as in the case of Pt/Al_2O_3 catalyst, the decomposition of CH_x species adsorbed on the catalyst (Fig. 4C) surface toward CO and H_2 (Eq. (10)) cannot be excluded.

Increasing temperature above ca 250 °C results in a decrease of CO concentration, which is accompanied by evolution of CO_2 due to the WGS reaction. Carbon monoxide concentration remains at low levels in the wide temperature range of 300–440 °C and then increases, probably due to the reaction of dry methane reforming (Eq. (13)), as witnessed by the consumption of CH_4 and evolution of CO and H_2 above 450 °C.

The detection of acetaldehyde in the temperature range of 300–400 °C, in association with the increasing CH_4 concentration up to 370 °C, indicates that acetaldehyde (Eq. (5)) or ethanol (Eq. (3)) decomposition reactions may also take place. Carbon dioxide consumption above 500 °C is probably due to the reverse WGS reaction. The considerable increase of CO and H_2 concentrations at temperatures above 500 °C is due to steam reforming of ethanol (Eq. (14)).

Comparison of the results of Fig. 5A, B and C shows that at low temperatures (200–300 °C) hydrogen production is significantly higher when Pt is supported on ZrO_2 and Al_2O_3 rather than on CeO_2, which agrees well with the results discussed above under steady reaction conditions. In all cases, the detection of methane takes place in the same temperature range, with its amount being more or less similar for all catalysts investigated. Although no such evidence is provided by comparing CO evolution (due to its participation in WGS reaction), the above behavior indicates that the observed differences in H_2 selectivity are not related to the different catalyst reactivity toward ethanol decomposition reaction. Regarding acetaldehyde production, it elutes at lower temperatures and in higher amounts over Pt/CeO_2 catalyst, implying that ethanol dehydrogenation reaction is affected by the nature of the support and is enhanced over the latter catalyst. However, DRIFTS spectra of Fig. 3C show that decomposition of acetyl species, produced via acetaldehyde dehydrogenation, is favored over Pt/ZrO_2 catalyst. It may then be suggested that ethanol dehydrogenates toward acetaldehyde over the most active Pt/ZrO_2 catalyst, followed by its fast dehydrogenation toward acetyl species and thus, resulting in the detection of lower amount of acetaldehyde in the gas phase.

It is of interest to note that the onset and the extent of the WGS reaction is significantly affected by the nature of the support. In the case of Pt/ZrO_2 catalyst (Fig. 5C) the WGS reaction is initiated at lower temperatures (around 90 °C lower) and CO concentration remains in its minimum value for a wider temperature range compared to Pt/CeO_2 catalyst (Fig. 5B). In the case of Pt/Al_2O_3 catalyst, although the consumption of CO is initiated already at 280 °C, its concentration remains at high levels leading to the production of lower amounts of CO_2. The above results demonstrate the enhancement of the WGS reaction over the Pt/ZrO_2 catalyst and agree well with the results of Fig. 2B.

Comparison of DRIFTS (Fig. 3) with transient-MS (Fig. 5) spectra demonstrates that the main reaction pathway for ethanol reforming at low temperatures over the platinum supported catalyst is the ethanol dehydrogenation, through the formation of surface ethoxy species and subsequent acetaldehyde, which is further decomposed toward methane, hydrogen and carbon oxides. The ability of the catalyst to enhance the WGS reaction results in significant variations in the population of adsorbed surface species and in the gas phase product distribution.

3.3.3. *Titration of carbon deposited on the catalysts under transient reaction conditions*

As discussed previously, one of the major problems in ethanol steam reforming reaction is related to coke formation on the catalyst surface, which may take place via the "Boudouard" reaction, methane decomposition and/or cracking of ethylene produced by dehydration of ethanol. The amount of carbon deposited on the catalyst surface was estimated by TPO, which was performed immediately after completions of the experiments shown in Fig. 5. As observed in Fig. 6A, the profile of CO_2 thus produced from the Pt/Al_2O_3 sample exhibits three peaks with maxima at about 325, 495 (shoulder) and 570 °C, indicating that there are three distinct carbon species on the catalyst surface. One of these can be attributed to polymeric carbon originating from ethylene decomposition, which was found to be produced between 200 and 300 °C [2,7,51]. Regarding the other carbon species, they may be due to decomposition of CH_x species, which was found to be present on the catalyst surface (Fig. 3B) [8,51].

In Table 2, the amounts ($\mu mol\ m^{-2}$) of CO_2 produced and O_2 consumed during TPO experiments are presented for all catalysts investigated. The amount of carbon deposited on the Pt/Al_2O_3 catalyst during TPSR experiment was estimated to be 0.7 $\mu mol\ m^{-2}$. Qualitatively similar results were obtained for Pt/CeO_2 catalyst, the CO_2 profile of which (Fig. 6A) consists, as in the case of Pt/Al_2O_3, of three peaks with maxima at about 160, 250 and 373 °C. The amount of CO_2 produced is significantly higher (8.7 $\mu mol\ m^{-2}$) and evolved at lower temperatures compared to that obtained from Pt/Al_2O_3 catalyst. This indicates that carbon deposition is enhanced over Pt/CeO_2 catalyst, but its oxidation occurs at lower temperatures. Regarding Pt/ZrO_2 catalyst the amount of carbon deposited was found to be 0.3 $\mu mol\ m^{-2}$. Results of Table 2 show that carbon deposition during ethanol steam reforming reaction decreases following the order $CeO_2 >> Al_2O_3 > ZrO_2$. The significantly higher carbon formation over Pt/CeO_2 catalyst may be related with the higher production of ethylene under ethanol steam reforming conditions (Fig. 5B). Carbon dioxide evolution at higher temperatures over Pt/Al_2O_3 catalysts

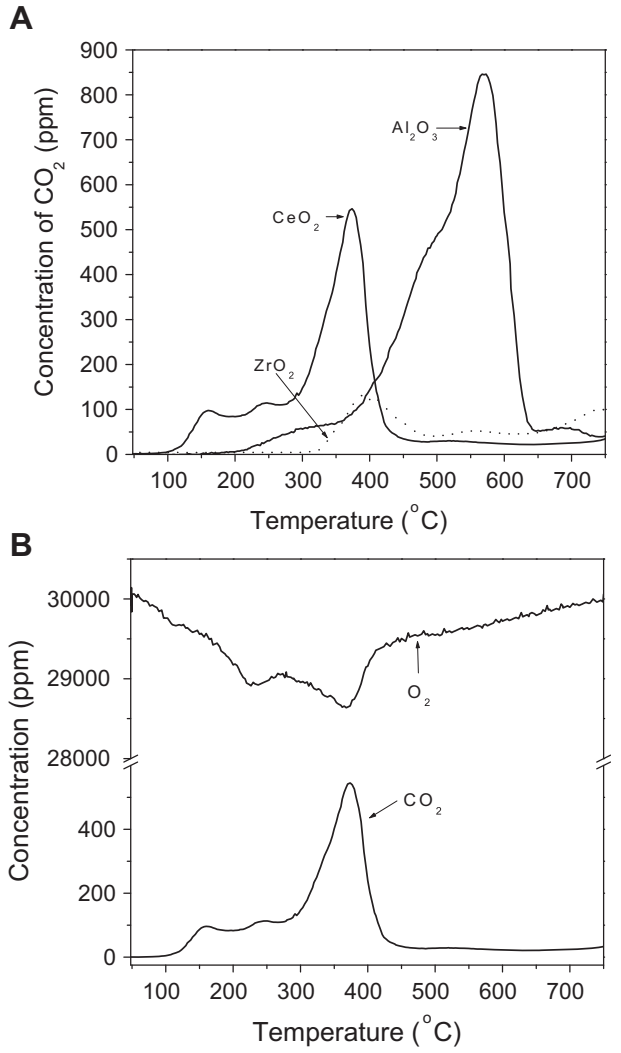

Fig. 6 – (A) Responses of CO_2 produced during temperature-programmed oxidation with 3%O_2 (in He) occurred immediately after the TPSR experiments of Fig. 5 over supported Pt catalysts. (B) Responses of CO_2 and O_2 recorded during TPO experiment over Pt/CeO_2 catalyst.

indicates that carbon formation on the surface of this catalyst is more stable compared to the other samples investigated.

It is of interest to note that in all cases the consumption of O_2 is significantly higher compared to CO_2 production (by a factor of 2, 6 and 8 for Al_2O_3, CeO_2 and ZrO_2, respectively) (Table 2). This is clearly shown in Fig. 6B, where the responses of O_2 and CO_2 recorded during TPO experiment are presented as a function of temperature for Pt/CeO_2 catalyst. Results indicate that oxidation of surface carbon, according to Eq. (16) is not the only oxygen consumption mechanism. A significant part of oxygen is consumed for the oxidation of CH_x species (Eq. (17)), as well as for the oxidation of the metal oxide carrier (Eq. (18)), which may be reduced by H_2 produced during ethanol reforming reaction.

Table 2 – Amounts of O_2 consumed and CO_2 produced during TPO experiments.

Catalyst	Amount of O_2 consumed (μmol m^{-2})	Amount of CO_2 produced (μmol m^{-2})
0.5%Pt/Al_2O_3	1.4	0.7
0.5%Pt/CeO_2	52.8	8.7
0.5%Pt/ZrO_2	2.2	0.3

$$C + O_2 \rightarrow CO_2 \quad (16)$$

$$CH_x + \frac{4+x}{2}O_2 \rightarrow CO_2 + \frac{x}{2}H_2O \quad (17)$$

$$CeO_{2-x} - x + \frac{x}{2}O_2 \rightarrow CeO_2 \quad (18)$$

The latter reaction may be responsible for oxygen consumption which takes place at low temperatures (100–300 °C) over Pt/CeO_2 catalyst (Fig. 6B).

The overall carbon balance of the TPSR experiments has been calculated using Eq. (19). The amount of carbon deposited on the catalyst surface, calculated by TPO experiments has been also taken into account.

$$[\text{Carbon}]_{\text{total}} = \frac{[CO] + [CO_2] + [CH_4]}{2} + [C_2H_5OH] + [CH_3CHO] + [C_2H_4] \quad (19)$$

In all cases examined the carbon balance is satisfactory, with deviation equal to 5–10%.

4. Conclusions

Results of the present study show that catalytic performance of supported platinum catalysts for the steam reforming of ethanol at low temperatures depends on the nature of the metal oxide support. Platinum catalysts exhibit higher activity and selectivity toward hydrogen when supported on Al_2O_3 or ZrO_2 rather than on CeO_2 carrier. Ethanol decomposition and dehydrogenation reactions are enhanced at low temperatures, whereas reforming, water-gas shift, and methanation reactions dominate at higher temperatures. The oxidation state of Pt seems to affect catalytic activity, which was found to decrease with increasing the population of adsorbed CO species on partially oxidized ($Pt^{\delta+}$) sites. Results of TPSR and DRIFT experiments provide evidence that the key step for ethanol reforming at low temperatures is ethanol dehydrogenation reaction, producing surface ethoxy species and subsequent acetaldehyde, which is further decomposed toward methane, hydrogen and carbon oxides. The ability of the catalyst to enhance the WGS reaction results in significant variations in the population of adsorbed surface species and in gas phase product distribution. Carbon deposition on the surface of all catalysts investigated is taking place under ethanol steam reforming conditions. However, during TPO experiments oxygen is consumed not only to oxidize surface carbon, but also CH_x species accumulated on the catalyst surface as well as the metal oxide carrier, which may be reduced by H_2 produced during ethanol reforming reaction.

Acknowledgments

This research has been co-financed by the European Union (European Social Fund – ESF) and Greek national funds through the Operational Program "Education and Lifelong Learning" of the National Strategic Reference Framework (NSRF)-Research Funding Program: Thales. Investing in knowledge society through the European Social Fund (CAT-BIOFUEL project).

REFERENCES

[1] Ghenciu AF. Review of fuel processing catalysts for hydrogen production in PEM fuel cell systems. Curr Opin Solid State Mater Sci 2002;6:389–99.
[2] Fatsikostas AN, Kondarides DI, Verykios XE. Production of hydrogen for fuel cells by reformation of biomass-derived ethanol. Catal Today 2002;75:145–55.
[3] Liguras DK, Kondarides DI, Verykios XE. Production of hydrogen for fuel cells by steam reforming of ethanol over supported noble metal catalysts. Appl Catal B 2003;43: 345–54.
[4] Klouz V, Fierro V, Denton P, Katz H, Lisse J, Bouvot-Mauduit S, et al. Ethanol reforming for hydrogen production in a hybrid electric vehicle: process optimisation. J Power Sources 2002;105:26–34.
[5] Deluga GA, Salge JR, Schmidt LD, Verykios XE. Renewable hydrogen from ethanol by autothermal reforming. Science 2004;303:993–7.
[6] Sanchez-Sanchez MC, Navarro RM, Fierro JLG. Ethanol steam reforming over $Ni/M_xO_y–Al_2O_3$ (M=Ce, La, Zr and Mg) catalysts: influence of support on the hydrogen production. Int J Hydrogen Energy 2007;32:1462–71.
[7] Basagiannis AC, Panagiotopoulou P, Verykios XE. Low temperature steam reforming of ethanol over supported noble metal catalysts. Top Catal 2008;51:2–12.
[8] Szijjarto GP, Tompos A, Margitfavi JL. High-throughput and combinatorial development of multicomponent catalysts for ethanol steam reforming. Appl Catal A 2010;1-2:417–26.
[9] Panagiotopoulou P, Kondarides DI. Effect of morphological characteristics of TiO_2-supported noble metal catalysts on their activity for the water-gas shift reaction. J Catal 2004; 225:327–36.
[10] Panagiotopoulou P, Kondarides DI, Verykios XE. Selective methanation of CO over supported Ru catalysts. Appl Catal B 2009;88:470–8.
[11] Panagiotopoulou P, Kondarides DI, Verykios XE. Chemical reaction engineering and catalysis issues in distributed power generation systems. Ind Eng Chem Res 2011;50: 523–30.
[12] Sun J, Qiu XP, Wu F, Zhu WT. H_2 from steam reforming of ethanol at low temperature over Ni/Y_2O_3, Ni/La_2O_3 and Ni/Al_2O_3 catalysts for fuel-cell application. Int J Hydrogen Energy 2005;30:437–45.
[13] Raskó J, Dömök M, Baán K, Erdőhelyi A. FTIR and mass spectrometric study of the interaction of ethanol and ethanol–water with oxide-supported platinum catalysts. Appl Catal A 2006;299:202–11.
[14] Ciambelli P, Palma V, Ruggiero A. Low temperature catalytic steam reforming of ethanol. 1. The effect of the support on the activity and stability of Pt catalysts. Appl Catal B 2010;96: 18–27.
[15] Comas J, Marino F, Laborde M, Amadeo N. Bio-ethanol steam reforming on Ni/Al_2O_3 catalyst. Chem Eng J 2004;98:61–8.
[16] Diagne C, Idriss H, Kiennemann A. Hydrogen production by ethanol reforming over $Rh/CeO_2–ZrO_2$ catalysts. Catal Commun 2002;3:565–71.
[17] Ciambelli P, Palma V, Ruggiero A, Iaquaniello G. Low temperature catalytic steam reforming of ethanol. 2. Preliminary kinetic investigation of Pt/CeO_2 catalysts. Appl Catal B 2010;96:190–7.
[18] Shi Q, Liu C, Chen W. Hydrogen production from steam reforming of ethanol over $Ni/MgO-CeO_2$ catalyst at low temperature. J Rare Earths 2009;27:948–54.
[19] Sun J, Qiu X, Wu F, Zhu W, Wang W, Hao S. Hydrogen from steam reforming of ethanol in low and middle temperature range for fuel cell application. Int J Hydrogen Energy 2004;29: 1075–81.
[20] Llorca J, Homs N, Sales J, Ramírez de la Piscina P. Efficient production of hydrogen over supported cobalt catalysts from ethanol steam reforming. J Catal 2002;209:306–17.
[21] Llorca J, Ramírez de la Piscina P, Dalmon J-A, Sales J, Homs N. CO-free hydrogen from steam-reforming of bioethanol over ZnO-supported cobalt catalysts. Effect of the metallic precursor. Appl Catal B 2003;43:355–69.
[22] Llorca J, Homs N, Sales J, Fierro JLG, Ramírez de la Piscina P. Effect of sodium addition on the performance of Co-ZnO-based catalysts for hydrogen production from bioethanol. J Catal 2004;222:470–80.
[23] Torres JA, Llorca J, Casanovas A, Domínguez M, Salvadó J, Montané D. Steam reforming of ethanol at moderate temperature: multifactorial design analysis of $Ni/La_2O_3-Al_2O_3$, and Fe- and Mn-promoted Co/ZnO catalysts. J Power Sources 2007;169:158–66.
[24] Casanovas A, Leitenburg C, Trovarelli A, Llorca J. Catalytic monoliths for ethanol steam reforming. Catal Today 2008; 138:187–92.
[25] Zhang B, Tang X, Li Y, Xu Y, Shen W. Hydrogen production from steam reforming of ethanol and glycerol over ceria-supported metal catalysts. Int J Hydrogen Energy 2007;32: 2367–73.
[26] Erdőhelyi A, Raskó J, Kecskés T, Tóth M, Dömök M, Baán K. Hydrogen formation in ethanol reforming on supported noble metal catalysts. Catal Today 2006;116:367–76.
[27] Dömök M, Tóth M, Raskó J, Erdőhelyi A. Adsorption and reactions of ethanol and ethanol–water mixture on alumina-supported Pt catalysts. Appl Catal B 2007;69: 262–72.
[28] Lima SM, Silva AM, Cruz IO, Jacobs G, Davis BH, Mattos LV, et al. Hydrogen production through steam reforming of ethanol over Pt/ZrO_2, Pt/CeO_2 and $Pt/CeZrO_2$ catalysts. Catal Today 2008;138:162–8.
[29] Panagiotopoulou P, Kondarides DI. Effect of the nature of the support on the catalytic performance of noble metal catalysts for the water-gas shift reaction. Catal Today 2006; 112:49–52.
[30] Panagiotopoulou P, Kondarides DI. A comparative study of the water-gas shift activity of Pt catalysts supported on single (MO_x) and composite (MO_x/Al_2O_3, MO_x/TiO_2) metal oxide carriers. Catal Today 2007;127:319–29.
[31] Ciambelli P, Palma V, Ruggiero A, Iaquaniello G. Platinum catalysts for the low temperature catalytic steam reforming of ethanol. Chem Eng Trans 2009;17:19–24.
[32] Vignatti CI, Avila MS, Apesteguía CR, Garetto TF. Study of the water-gas shift reaction over Pt supported on CeO_2-ZrO_2 mixed oxides. Catal Today 2011;171:297–303.
[33] Azzam KG, Babich IV, Seshan K, Lefferts L. Bifunctional catalysts for single-stage water-gas shift reaction in fuel cell applications. Part 1. Effect of the support on the reaction sequence. J Catal 2007;251:153–62.
[34] Panagiotopoulou P, Christodoulakis A, Kondarides DI, Boghosian S. Particle size effects on the reducibility of

titanium dioxide and its relation to the water-gas shift activity of Pt/TiO_2 catalysts. J Catal 2006;240:114–25.
[35] Lundie DT, McInroy AR, Marshall R, Winfield JM, Jones P, Dudman CC, et al. Improved description of the surface acidity of n-Alumina. J Phys Chem B 2005;109:11592–601.
[36] Sanchez-Sanchez MC, Navarro Yerga RM, Kondarides DI, Verykios XE, Fierro JLG. Mechanistic aspects of the ethanol steam reforming reaction for hydrogen production on Pt, Ni, and PtNi catalysts supported on γ-Al_2O_3. J Phys Chem A 2010; 114:3873–82.
[37] Primet M. Electronic transfer and ligand effects in the infrared spectra of adsorbed carbon monoxide. J Catal 1984; 88:273–82.
[38] Panagiotopoulou P, Papavasiliou J, Avgouropoulos G, Ioannides T, Kondarides DI. Water-gas shift activity of doped Pt/CeO_2 catalysts. Chem Eng J 2007;134:16–22.
[39] Tanaka K, White JM. Infrared studies of CO adsorption on reduced and oxidized $PtTiO_2$. J Catal 1983;79:81–94.
[40] Lane GS, Wolf EE. Characterization and Fourier transform infrared studies of the effects of TiO_2 crystal phases during CO oxidation on $PtTiO_2$ catalysts. J Catal 1987;105:386–404.
[41] Liu Z, Li X, Chen Z, Ying P, Feng Z, Li C. Effect of reduction method on the surface states of Pt/Al_2O_3. J Fuel Chem Technol 2009;37:205–11.
[42] Hertl W, Cuenca AM. Infrared kinetic study of reactions of alcohols on the surface of alumina. J Phys Chem 1973;77: 1120–6.
[43] Shimizu K, Kawabata H, Satsuma A, Hattori T. Formation and reaction of surface acetate on Al_2O_3 during NO reduction by C_3H_6. Appl Catal B 1998;19:L87–92.
[44] Yee A, Morrison SJ, Idriss H. A study of ethanol reactions over Pt/CeO_2 by temperature-programmed desorption and in situ FT-IR spectroscopy: evidence of Benzene Formation. J Catal 2000;191:30–45.
[45] Lima SM, Silva AM, Costa LOO, Graham UM, Jacobs G, Davis BH, et al. Study of catalyst deactivation and reaction mechanism of steam reforming, partial oxidation, and oxidative steam reforming of ethanol over Co/CeO_2 catalyst. J Catal 2009;268:268–81.
[46] Jacobs G, Patterson PM, Graham UM, Crawford AC, Davis BH. Low temperature water gas shift: the link between the catalysis of WGS and formic acid decomposition over Pt/ceria. Int J Hydrogen Energy 2005;30:1265–76.
[47] Mattos LV, Noronha FB. Hydrogen production for fuel cell applications by ethanol partial oxidation on Pt/CeO_2 catalysts: the effect of the reaction conditions and reaction mechanism. J Catal 2005;233:453–63.
[48] Yee A, Morrison SJ, Idriss H. A study of the reactions of ethanol on CeO_2 and Pd/CeO_2 by steady state reactions, temperature programmed desorption, and *in situ* FT-IR. J Catal 1999;186:279–95.
[49] Mavrikakis M, Barteau MA. Oxygenate reaction pathways on transition metal surfaces. J Mol Catal A: Chem 1998;131: 135–47.
[50] Dömök M, Oszkó A, Baán K, Sarusi I, Erdőhelyi A. Reforming of ethanol on Pt/Al_2O_3-ZrO_2 catalyst. Appl Catal B 2010;383: 33–42.
[51] Fatsikostas AN, Verykios XE. Reaction network of steam reforming of ethanol over Ni-based catalysts. J Catal 2004; 225:439–52.